Effect of Irrigated Agriculture on Low-level Cloud in the Chukurova Plain, Turkey

Toshichika Iizumi[1], Toshihisa Fujiwara[1], Takehiro Yuyama[2], and Fujio Kimura[3]
[1] *Graduate School of Life and Environmental Sciences, University of Tsukuba,*
[2] *Master's Program in Environmental Sciences, University of Tsukuba*
[3] *Terrestrial Environment Research Center, University of Tsukuba*
1-1-1 Tennodai, Tsukuba, 305-8572, Japan

1. Introduction

Southern Turkey is dominated by the Mediterranean climate. Precipitation in summer is less 50 mm/month (Turkes, 1996). However, Chukurova Plain, which locates lower Seyhan River Basin, is often covered by low-level clouds even in dry summer season (Fig. 1).

The observed clouds are expected to be shallow cumulus clouds, and these clouds are sensitive to land surface condition in comparison with high-level clouds. In Chukurova Plain, current water consumption for agricultural irrigation reaches to 440 million m^3 during August (Nagano and Donma, 2004). Since total irrigated croplands is 90 thousands ha (Kameysma, 2004), the irrigation water fed to a unit square cropland can be estimated to 489.8 mm/month (= 15.8 mm/day). This amount of irrigated water is comparable to 70% of the annual precipitation in this area. Considering such background, the clouds may be affected by the large-scaled and intensive irrigation. Thus, this study aims to reveal the effect of irrigated agriculture on the clouds by using a Regional Climate Model (RCM).

2. Data and methods

2.1. Satellite image data

The satellite images are used to validate the reproductivity of the RCM as an observational data. The Moderate Resolution Imaging spectrometer (MODIS) data were obtained from the MODIS Rapid Response System (NASA/GSFC, 2006). Adapted data is the near-real-time true-color products in the archive of the "AERONET_IMS-METU_ERDEMLI" Subset. The subset covers southern Turkey with a 250m spatial resolution. The satellites of Terra and Aqua observed Chukurova Plain once a day; the Terra observes in a morning, mostly at 1000 Local Standard Time (LST) to 1200 LST; the Aqua observes in an early afternoon, mostly at 1200 LST to 1430 LST.

2.2. Numerical experiments

A RCM (TERC-RAMS) was adapted to reproduce the clouds and to simulate the effect of irrigated agriculture. The TERC-RAMS is a version of the Regional Atmospheric Modeling System modified by the Terrestrial Environmental Research Center, University of Tsukuba (Sato and Kimura, 2005). The RCM has a two-way nested grid system; the outer domain covers Turkey with a grid interval of 16 km; the middle one covers entire Chukurova Plain with a grid interval of 4 km; the innermost one covers western part of the plain with a grid interval of 1 km (Fig. 2). Every domain includes 46 layers in the terrain following vertical coordinate system. The lowest layer is located 90 m up from the screen height. The RCM used no convective parameterization in the innermost domain, thus the model works as a cloud resolution model.

Two sensitivity analysis was conducted; (1) the actual land-use ("CTL-run"), the land-use data was given by the 30 second grid land cover and land use data of the U.S. Geological Survey (USGS); (2) the spatially-uniform short grass ("UNI-run"). The soil types are silt roam in both runs.

The initial boundary conditions for the outer domain were fed by the global reanalysis data provided by the National Center for Environmental Prediction/National Center for Atmospheric Research (NCEP/NCAR) and monthly mean sea surface temperature (Reynolds et al., 2002). The integration period is 23 hours from 2100 LST in 6 August to 2000 LST in 7 August, 2004.

3. Results

3.1. Validation of the reproductivity in the RCM

The model simulates the spatial pattern of clouds comparatively well. At the snap shot of 1100 LST in the model, the simulated clouds along the east coast of the plain agree with those observed by the satellite (Fig. 3). The model also simulates the clouds in western plain fairly well; however, the simulated clouds are less than those in the satellite image. In addition, the model fails to simulate the haze, which distributed the entire plain. At 1200 LST in the model, the model simulates well the clouds distributed along the western coast.

The model also simulates the diurnal change of the clouds (no figure); the diurnal change is derived from the sea breeze, and the simulated change agrees well with the results of continuous photographic observation from the ground surface (Iizumi et al., 2005).

3.2. Effects of irrigation agriculture on low-level clouds

At 0900 LST in the model, the amount of simulated clouds in the CTL-run is significantly greater than that in the UNI-run (Fig. 4). The result in the CTL-run shows much clouds in western and eastern part of plain, and the area around the lake created by the dam. The spatial pattern of the clouds in the CTL-run agrees with that of irrigated cropland (no figure). Such tendency is consistently observed in before noon in the model; however, the difference between two runs becomes unclear in afternoon.

4. Discussion

As the mechanism of the low-level clouds enhancement, following factors are assumed to play important roles i.e., (1) the supply of water vapor from the irrigated croplands to the atmosphere through evapotranspiration; (2) the strong sensible heat flux from the ground surface derived from sufficient radiation. Since, the factors enhance the depth of the mixed layer and height of thermals, then, the clouds are formed at the top of the thermals. However, the result in UNI-run shows that the clouds in southern plain appear even in drier land surface condition. It suggests that the clouds in Chukurova Plain are formed by multiple mechanisms depending on the area.

5. Conclusion

The RCM simulates well the characteristics of the low-level clouds in spatial pattern and diurnal change. The spatial pattern of the clouds in before noon agrees with that of irrigated cropland. Thus, large-scaled and intensive irrigated agriculture is certainly one of factors to form the clouds. However, simulation results suggest that the clouds are formed by other mechanisms as well the irrigation depending on the area in the plain.

6. References

Iizumi, T., T. Fujiwara, and F. Kimura, 2005: Consecutive photographic observation of the low-level clouds covering over Chukurova Plain in summer, In: The Progress Report of ICCAP, 19-20.

Kameyama, H., 2004: The climate change impact on cropping pattern, In: The Interim Report of ICCAP, RIHN, Kyoto, 127-130.

Nagano, T., and S. Donma, 2004: Cropping pattern and water use in the Lower Seyhan irrigation Project, In: The Interim Report of ICCAP, RIHN, Kyoto, 93-96.

NASA/GSFC, 2006: MODIS Rapid Response System, In: http://rapidfire.sci.gsfc.nasa.gov.

Reynolds, R.W., N.A. Rayner, T.M. Smith, D.C. Stokes, and W. Wang, 2002: An improved in situ and satellite SST analysis for climate. *J. Climate*, 15, 1609-1625.

Sato, T., and F. Kimura, 2005: Diurnal cycle of convective instability around the central mountains in Japan during the warm season, *J. Atmos. Sci.*, 62, 1626-1636.

Turkes, M., 1996: Spatial and temporal analysis of annual rainfall variations in Turkey, *Int. J. Climatology*, 16**,** 1057-1076.

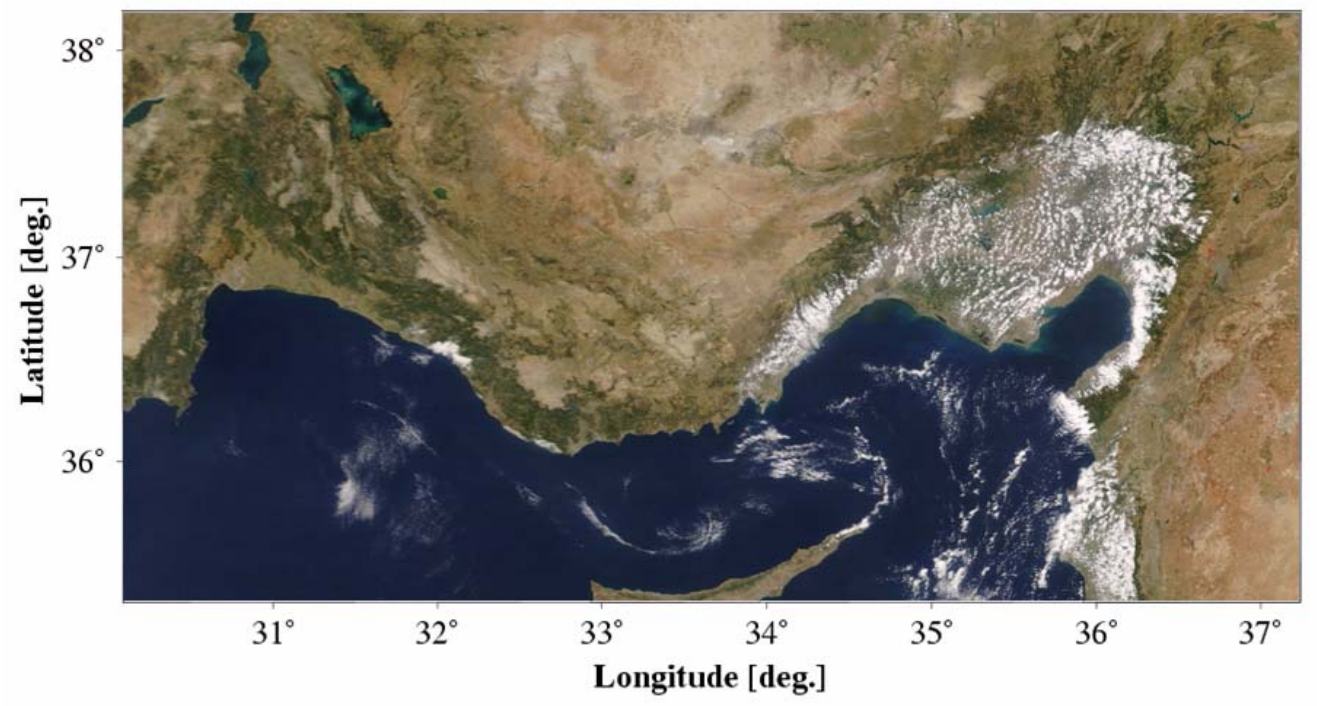

Fig. 1. Typical low-level clouds observed by the MODIS/Terra at 1008 LST (0808 UTC) on 01 July, 2005.

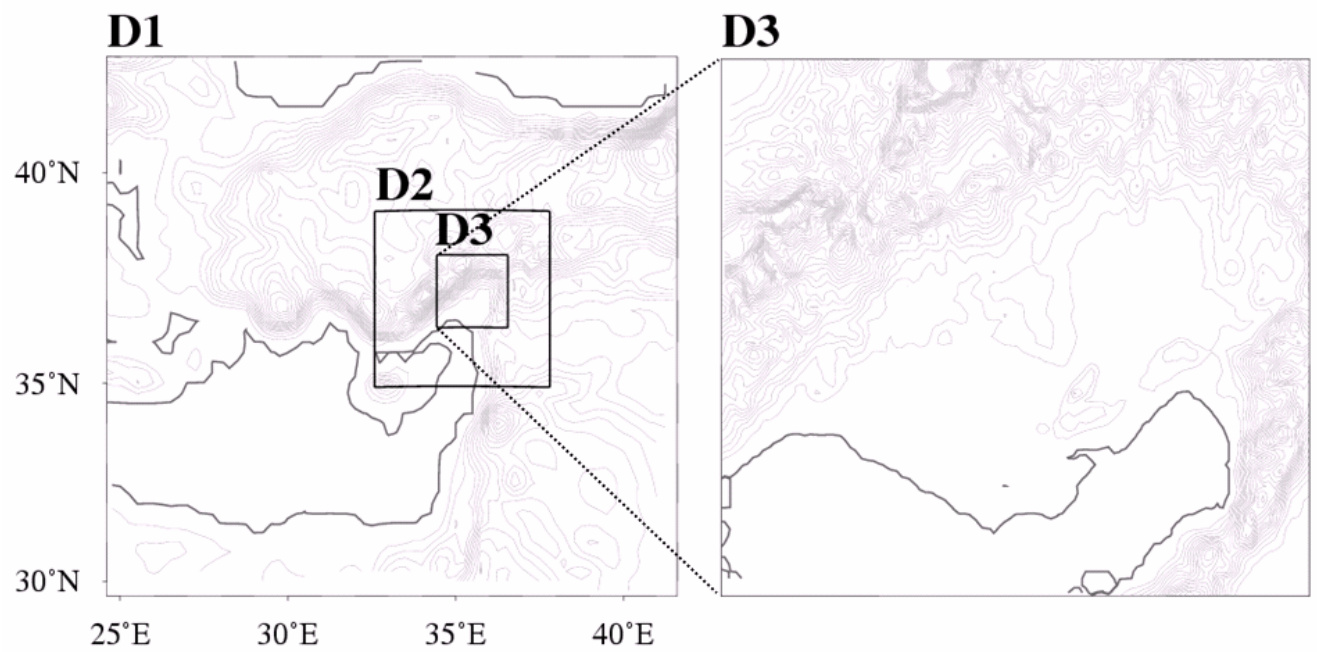

Fig. 2. RCM domains; the bold lines show elevation of 0 m in the RCM, while the thin lines show that of 100 m.

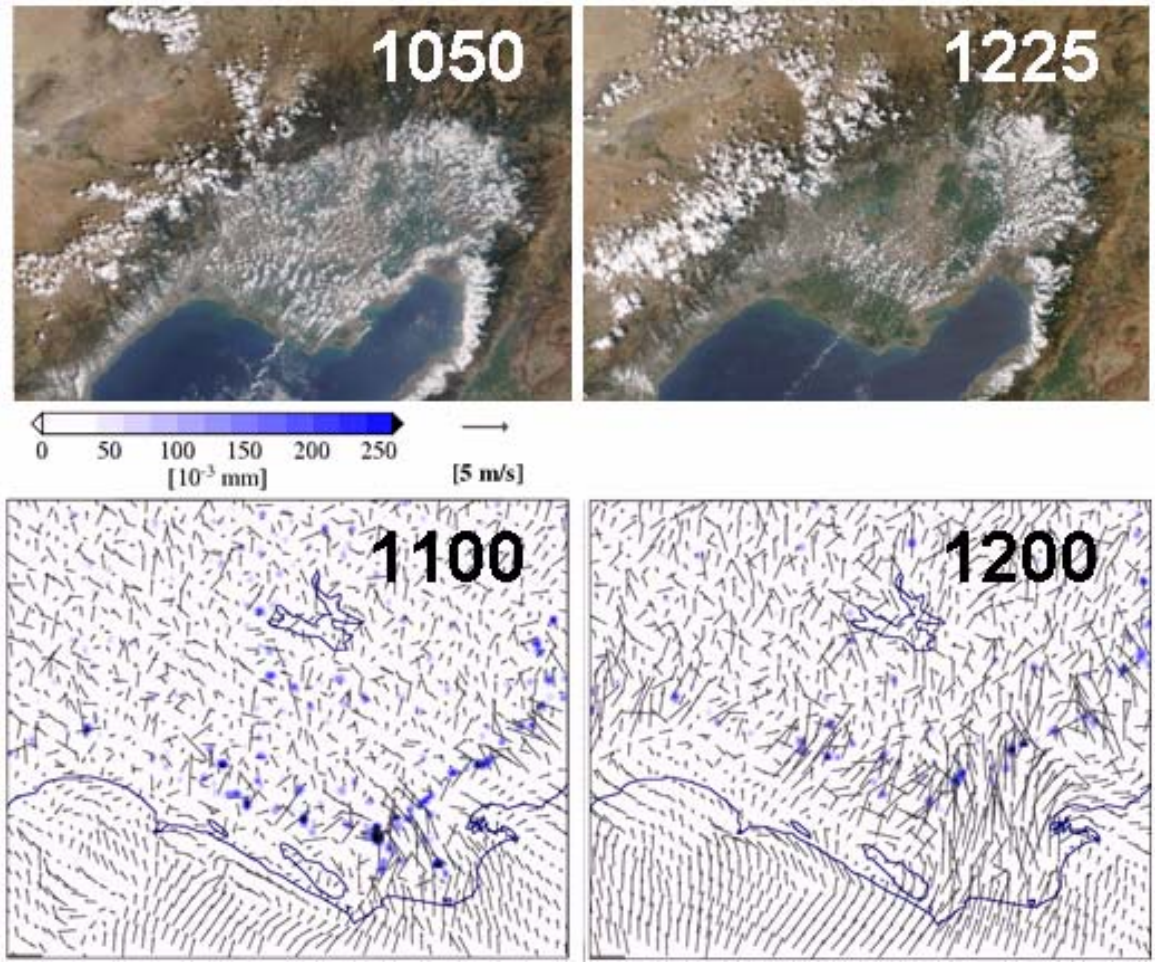

Fig. 3. Snap shots of clouds observed by the MODIS/Terra and Aqua at 1050 LST and 1225 LST on 07 August, 2004 (Top), and those of simulated clouds and wind systems at a height of 1100 m (bottom); The blue shades show the integrated cloud water amount (10^{-3} mm).

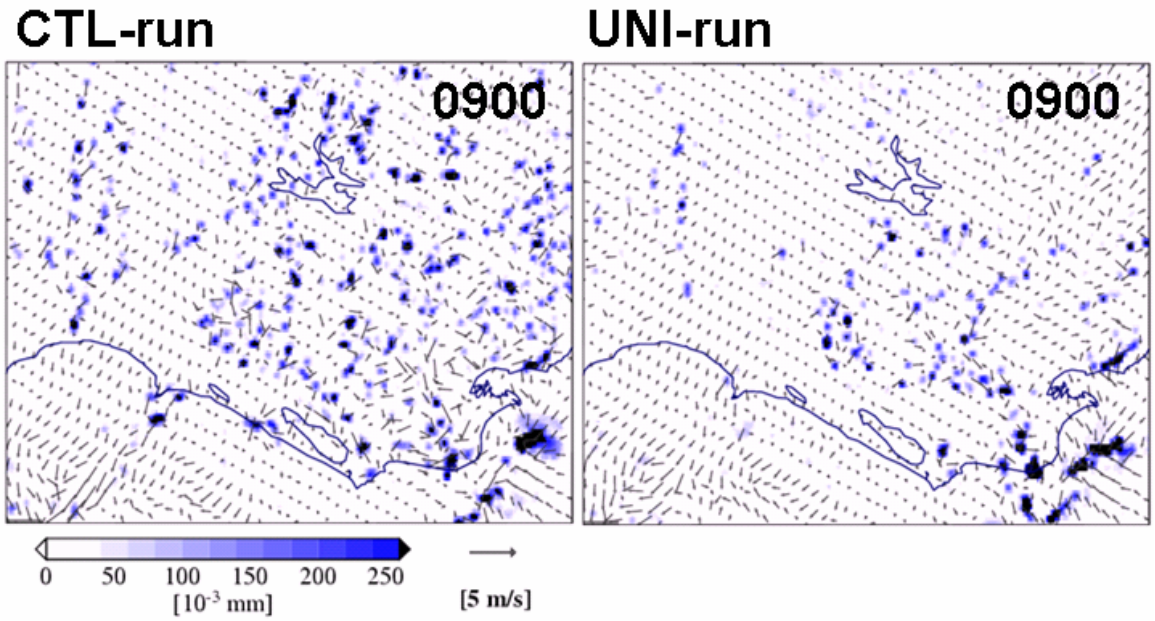

Fig. 4. Snap shots of simulated clouds and wind systems at height of 1100 m on 0900 LST in the CTL-run and UNI-run. The blue shades show the integrated cloud water amount (10^{-3} mm).

The Impacts of Climate Change on the Hydrology and Water Resources of the Seyhan River Basin, Turkey

Hydrology and Water Resources Sub-Group
Katsuyuki FUJINAWA[1], Kenji TANAKA[2], Yoichi FUJIHARA[3], and Toshiharu KOJIRI[4]
[1]*Geo-Environmental Engineering, Faculty of Engineering, Shinshu University, 550 Wakasato, Nagano, Nagano 380-8533*
[2,4]*Disaster Prevention Research Institute, Kyoto University, Gokasho, Uji 611-0011*
[3]*Research Institute for Humanity and Nature, 457-4 Kamigamo-motoyama, Kita-Ku, Kyoto 603-8047*

1. Introduction

This report assesses the impacts of global warming on the hydrology and water resources of the Seyhan River Basin, Turkey. The ICCAP Hydrology and Water Resources sub-group consists of three groups focusing on (a) groundwater (Dr. Fujinawa, Shinshu University), (b) surface energy and the water balance (Dr. Tanaka, Kyoto University), and (c) water resources (Dr. Fujihara, RIHN). Although these groups act individually, they exchange data to integrate the hydrology subgroup (**Figure 1**).

Section 2 of this paper summarizes the methods used and results found by these groups. Conclusions and suggestions based on the results are described in Section 3. Detailed descriptions of each group follow this paper, as separate reports.

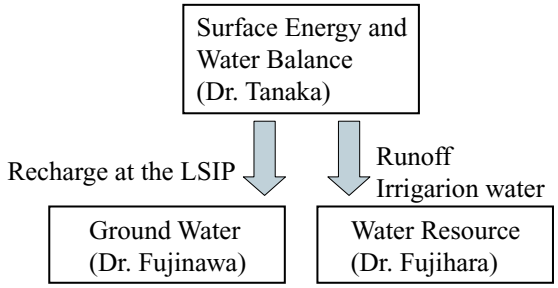

Fig.1 The ICCAP hydrology sub-group.

2. Methods and Results

2.1 Groundwater

A two-dimensional groundwater flow/mass transport model, referred to as the Saltwater Intrusion by Finite Elements and Characteristics (SIFEC) model, was developed and applied under various scenarios to assess the impacts of climate change on the subsurface water environment of the lower Seyhan River Basin (LSRB), Turkey.

Following calibration processes (**Figure 2** shows the current salinity distribution in the aquifer), projections for assessing the impacts of climate change on the subsurface water environment of the LSRB were performed for various scenarios based on adopted sea-level rise and climatic elements, irrigation practices, river runoff, and groundwater abstraction (see Fujinawa and Fujihara, 2007). Outputs of the projections are explained in terms of salinity of the Akyatan lagoon and groundwater, the groundwater table and velocity, salt accumulation on land, and water-logging. The results are summarized below.

The combination of sea-level rise by as much as 0.88 m/century, increasing evaporation, and reduced precipitation will cause a significant increase in salinity in the lagoon (**Figure 3**). Increased salinity in the lagoon will in turn deteriorate the groundwater quality. Groundwater salinity may drastically increase first beneath the lagoon (**Figure 4**) and then further inland in the aquifer.

The buildup of a high-saline zone in the aquifer beneath the lagoon could reduce the freshwater lens in the sand dune aquifer and also cause water-logging on the land surface (see sand dune area of **Figure 5**). Water-logging and increased salinity in shallow groundwater may cause severe accumulation of salt on the land surface.

Increasing evaporation, sea-revel rise, and increasing groundwater abstraction may all con-

tribute to salt accumulation. Thus, drainage measures are strongly recommended in the future to minimize the impacts of salt accumulation on the land surface. The groundwater table may decline significantly in accordance with enhanced groundwater abstraction (**Figure 5**).

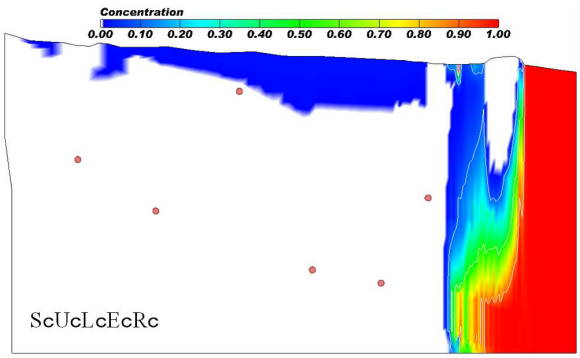

Fig.2 Distribution of salinity relative to Mediterranean.

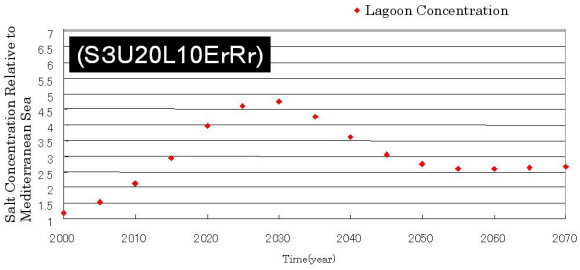

Fig.3 Temporal changes in the salinity of the lagoon water for scenario S3U20L10ErRr.

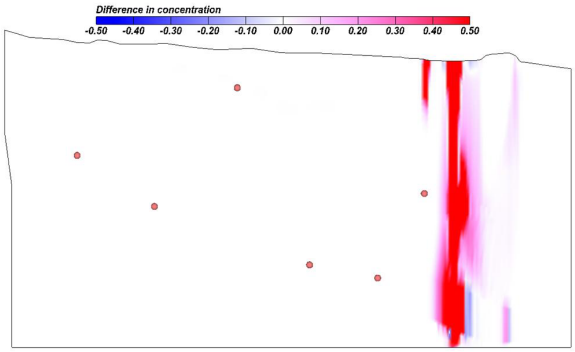

Fig.4 Difference in groundwater salinity between S3U20L10ErRr and control run.

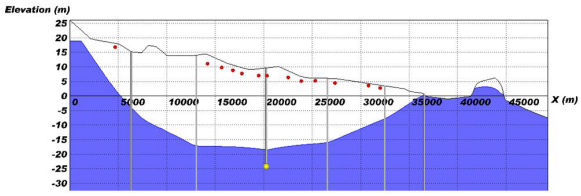

Fig.5 Location of groundwater table for scenario S3U20L10ErRr.

2.2 Surface Energy and Water Balance

Surface energy and water balance components and related hydrological variables of the Seyhan River Basin were estimated using an off-line simulation by the Land Surface Model (LSM) forced by the product of the Regional Climate Model (RCM) for both present and future (warm-up) conditions. The simulation period was from 1994 to 2003 for the present climate condition. For the future climate condition, two products were produced from different general circulation model (GCM) results (Meteorological Research Institute [MRI] and Center for Climate System Research [CCSR]). For the landcover condition, three land use scenarios (A0: no adaptation, A1: adaptation 1, A2: adaptation 2) were used. By combining climate conditions and land-use scenarios, six simulations were conducted for the future.

Maize and citrus were selected to represent irrigated crops. Based on information from the Irrigation and Drainage sub-group, the irrigation periods for maize and citrus were set as 23 May to 6 August and 14 May to 9 October, respectively. For the future climate simulation, the growing period was shortened by 10 days, considering faster plant growth under warmer conditions.

The SPOT VEGETATION Product and ECOCLIMAP database allow for good descriptions of the spatial distribution and time evolution of vegetation parameters. For consistency with the landcover condition, vegetation parameters were changed accordingly for the future land-use adaptation scenario by applying the average seasonal cycle for each vegetation class.

Figures 6-9 show the annual (10-year average) water balance components (precipitation, runoff, snowfall, maximum snow water equivalent [SWE]) for present and future climates (A0). Precipitation will decrease for the entire Seyhan basin, with particular reductions of more than 250 mm in the middle and delta regions. Maximum SWE is almost 0.4 Gt in the present climate but will decrease to as little as 0.1 Gt under the future climate (**Figure 10**). For the Seyhan delta (irrigated area), annual evaporation is about 800 mm, and about 500 mm of irrigation water must be supplied to maintain soil wetness during the growing

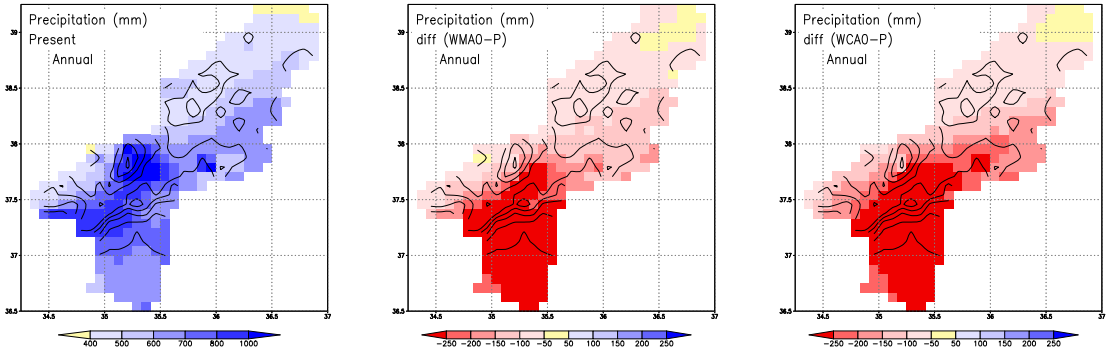

(a) Present (b) Diff(MRI) (c) Diff(CCSR)

Fig.6 Annual precipitation of present climate and its difference in MRI and CCSR run

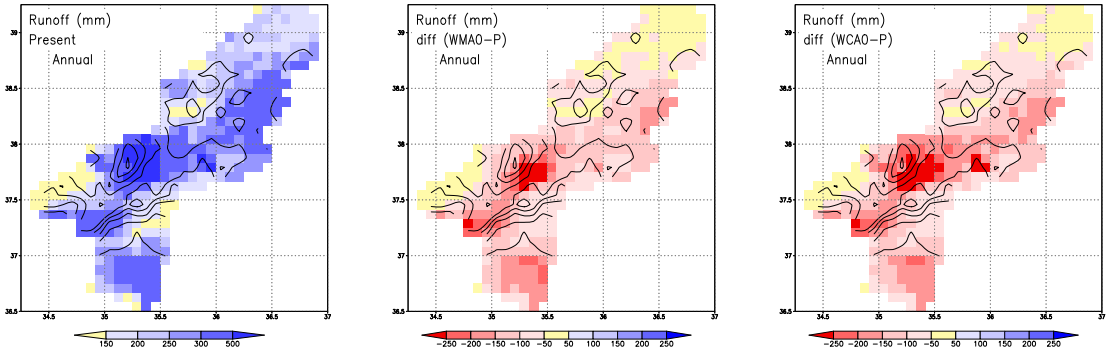

(a) Present (b) Diff(MRI) (c) Diff(CCSR)

Fig.7 Annual runoff of present climate and its difference in MRI and CCSR run

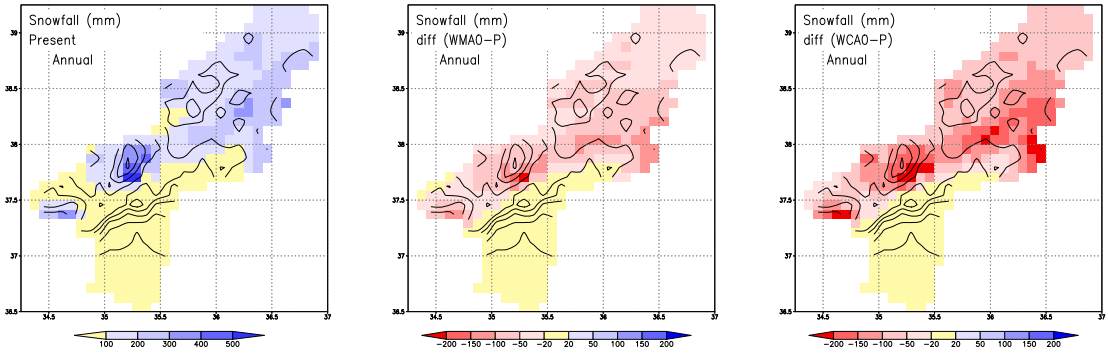

(a) Present (b) Diff(MRI) (c) Diff(CCSR)

Fig.8 Annual snowfall of present climate and its difference in MRI and CCSR run

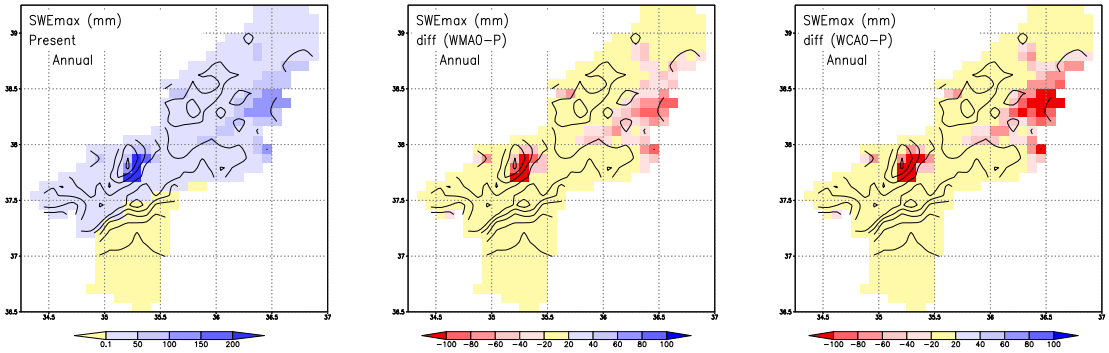

(a) Present (b) Diff(MRI) (c) Diff(CCSR)

Fig.9 Maximum SWE of present climate and its difference in MRI and CCSR run

Table 1 Basin average annual water balance components

unit:mm	Present	Future(A0)	Future(A1)	Future(A2)	diff(A0)	diff(A1)	diff(A2)
Prec	634.0	464.3	464.3	464.3	-169.7	-169.7	-169.7
Evap	411.3	373.9	365.4	378.9	-37.5	-45.9	-32.4
Runoff	281.6	168.9	168.1	170.4	-112.6	-113.5	-111.2
Irrig	53.8	69.7	60.4	76.4	15.9	6.6	22.5
delS	-5.0	-8.7	-8.8	-8.7	-3.7	-3.7	-3.6

season in the hot, dry summer. While precipitation will decrease over the whole basin, evaporation will increase in some parts. This coincides with the area of large SWE decreases. As a result of the reduced snow cover, those areas will receive more shortwave radiation (albedo effect). This increased energy will contribute to the increased evaporation in spring. Although the period for crop maturation will be shortened, the amount of irrigation water required is projected to increase because of the higher evaporation demand during the growing season and the reduction in soil moisture at the beginning of the growing period.

As a basin average, precipitation is projected to decrease by about 170 mm, while evapotranspiration and runoff will decrease by about 40 mm and 110 mm, respectively (**Table 1**). Considering the amount of the current water balance component, the impact on runoff is significantly large.

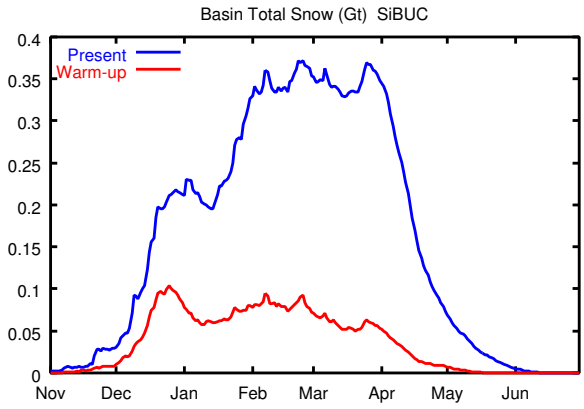

Fig.10 Basin total storage of snow.

2.3 Water Resources

The climate projected using two GCMs under the Special Report on Emissions Scenarios (SRES) A2 emissions scenario was used to drive hydrologic models to assess the impact of climate change on the water resources of the Seyhan River Basin. We used the Simple Biosphere including Urban Canopy (SiBUC) LSM to estimate the surface energy and water balance components. In addition, we employed the stream-flow routing model of Hydro-BEAM to simulate river discharge. We also developed reservoir models to simulate the reservoir operations of the Seyhan and Catalan dams.

The land and water use in the present period are the actual conditions in the Seyhan River Basin. For the future period, the following three scenarios were used: (a) Future: land and water use are the same as at present, (b) Adaptation 1: land and water use under low-investment conditions, and (c) Adaptation 2: land and water use under high-investment conditions. The results show the following.

Future inflow will decrease remarkably compared to that at present (**Figure 11**). In addition, decreases in April, May, and June inflow will be greater than those in other months, and the peak monthly inflow will occur earlier than at present.

The ratio of water withdrawal to discharge, which indicates the degree of water scarcity, is less than 0.4 at present (low water stress), but ranges from 0.4 to 0.7 in the future period and for Adaptation 1 (high water stress), and from 0.5 to 1.0 for Adaptation 2 (extremely high water stress).

The reservoir volume in the future and scenario 1 is less than at present, and in a few cases, the reservoir is empty (**Figure 12**). In contrast, in Adaptation 2, the reservoir is frequently empty. The reliabilities of the dams in the future and in Adaptation 1 range from 1 to 0.95 by the MRI and CCSR models. For Adaptation 2, the reliability ranges from 1 to 0.7 by the MRI and CCSR (**Figure 13**).

Although the ratio of water withdrawal to discharge will increase due to the effects of global warming (decreased discharge), it would be pos-

sible to meet water demands using the water resources system in the future case and in Adaptation 1. In contrast, the effects of global warming and the increased demand for water in the upper basin will lead to water scarcity for the Lower Seyhan Irrigation Project (LSIP) area in Adaptation 2.

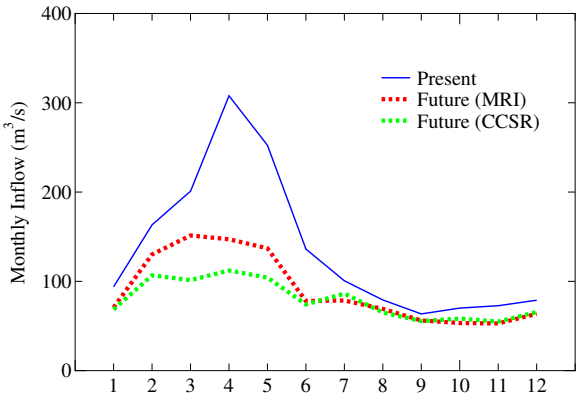

Fig.11 Stream flow changes predicted under different models.

3. Conclusions and Suggestions

The results suggest the following for the Seyhan River Basin:

1. The direct impacts of sea-level rise on salinity will not be serious. Nevertheless, the combination of sea-level rise, increasing evaporation, and reduced precipitation could cause a significant increase in salinity in the lagoon. Therefore, further groundwater abstraction will draw salt water.

2. The buildup of a high-saline zone in the aquifer beneath the lagoon could cause water-logging on the land surface. Water logging and increased salinity in shallow groundwater may cause salt accumulation on the land surface. The area planned for LSIP 4 will be unusable as irrigated land.

3. To minimize the impacts of salt accumulation on the land surface, drainage practices are strongly

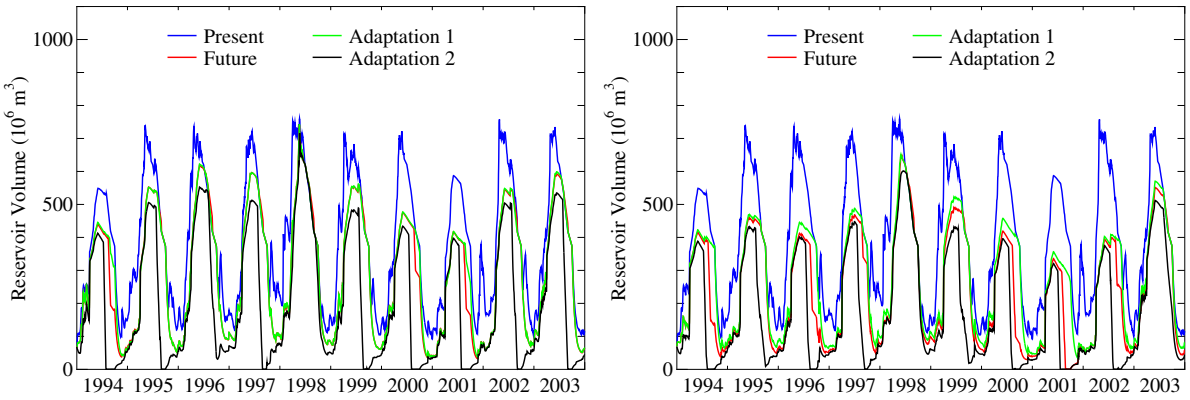

(a) MRI (b) CCSR

Fig.12 Reservoir changes.

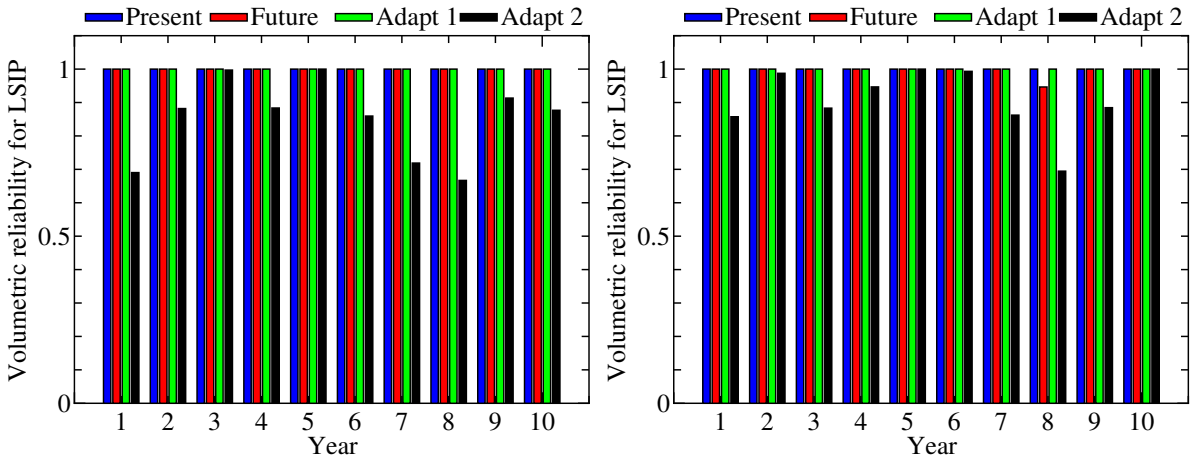

(a) MRI (b) CCSR

Fig.13 Reliability changes.

recommended in the future.

4. As a basin average, precipitation is projected to decrease by about 170 mm, while evapotranspiration and runoff will decrease by about 40 mm and 110 mm, respectively. Flood events will probably occur less frequently under global warming.

5. The expansion of irrigated land in the middle basin (increasing water demand) and the effects of global warming (decreasing river flow) will lead to water scarcity for the LSIP.

6. Quality control should be done to hydrological and meteorological data such as river flow, precipitation, temperature, and solar irradiation, and accurate databases should be created. In addition, attention should be paid to changes in these data to detect global warming and adapt to it.

7. Several observations should be made for mountainous areas. Snow should be observed and monitored on a daily basis. By observing the snow amount in winter, it is possible to forecast inflow, and it is relatively easy to operate reservoirs for flood control and water resource in the spring.

8. Forests will basically reduce river flow (increase transpiration). Therefore, in the case of an afforestation project, this effect should be considered.

References

Fujinawa, K., and Y. Fujihara (2007) Impacts of Climate Change on Subsurface Water Environment in the Lower Seyhan River Basin -Final Results of Calibration and Projection- (in this volume).